

SURVIVABILITY MODELING AND VALIDATION IN COMPLEX RIB-SKIN STRUCTURES

John Burkhardt, burkhard@usna.edu, Phone: 410-293-6507, Fax: 410-293-3041
Peter J. Joyce, pjoyce@usna.edu, Phone: 410-293-6533, Fax: 410-293-3041

Mechanical Engineering Department
United States Naval Academy
590 Holloway Road
Annapolis, MD 21402

Abstract

This paper presents a coordinated effort to model, test and validate the structural response of complex aerospace rib-skin structures in both undamaged and damaged configurations. Coordinated experimental and finite element model results are presented for cylindrical rib-skin structures each approximately nine foot long, and thirty inches in diameter. The test articles considered are of riveted aluminum construction and include internal structural components including bulkheads and complex stiffeners. Experimental reproduction of the highly idealized loading conditions used in the finite element models required the development of a custom loading rig that is described in detail. In summary, the finite element models were found to predict the structural stiffness of both the damaged and undamaged structures well for small deflections and strains. However, structural failure was not well predicted because large deflections and nonlinear material behavior were intentionally not modeled for simplicity.

Introduction

One of the greatest attractions of computer-aided engineering is its ability to cut costs and reduce design and analysis cycle times while simultaneously increasing quality. One example of this is the attempt to develop modeling and simulation methodologies for the assessment of structural survivability in aerospace structures. Such an undertaking is considerable because of the inherent complexity of the structures and loads involved. Additionally, confident deployment of any methods will require an extensive and rigorous program of model validation and physical testing.

With these larger goals in mind this paper presents a coordinated effort to model, test and validate the structural response of real aerospace rib-skin structures in both undamaged and damaged configurations. The structures considered were

approximately nine feet long, aluminum skinned cylinders thirty inches in diameter. The structural skin was riveted to z-shaped aluminum ribs and longerons. Additional internal structural components including bulkheads and complex stiffeners were present. All test articles were instrumented with strain gages and string potentiometers along the ventral axis of the cylinder and tested until failure in cantilever bending. Testing of the damaged structures required the development of a special cantilever bend rig that is described in detail below. In addition, high fidelity finite element models of the test articles were constructed and solved for pure cantilever bending. The finite element models were used in both the design of the experiment and construction of the test rig as well as to predict the structural response of both the damaged and undamaged structures.

Validation of computer simulations using physical testing obviously requires very close coordination between the ideal assumptions of the computer model and the physical constraints imposed during testing. For the finite element analyses performed in this study fixed translation and fixed rotation boundary conditions were imposed at the root-end of the specimens while a point-load of constant magnitude and direction was applied to the free-end. Normally, these boundary and loading conditions are easily reproduced in cantilever bend tests because deflections are small and the specimens possess symmetry about the line of action of the point load. In this study, however, of the five nominally axisymmetric test articles three of the five structures were damaged by the introduction of an irregularly shaped hole approximately 18 inches in diameter centered on one side. In addition, all five specimens were to be tested to failure with the expectation of large tip deflections. Consequently, significant tip deflections in both the lateral¹ and longitudinal¹ directions were anticipated in the damaged specimens. Tip deflections of this sort on a

¹ Perpendicular to the line of action of the point load.

REPORT DOCUMENTATION PAGE

Form Approved OMB No.
0704-0188

Public reporting burden for this collection of information is estimated to average 1 hour per response, including the time for reviewing instructions, searching existing data sources, gathering and maintaining the data needed, and completing and reviewing this collection of information. Send comments regarding this burden estimate or any other aspect of this collection of information, including suggestions for reducing this burden to Department of Defense, Washington Headquarters Services, Directorate for Information Operations and Reports (0704-0188), 1215 Jefferson Davis Highway, Suite 1204, Arlington, VA 22202-4302. Respondents should be aware that notwithstanding any other provision of law, no person shall be subject to any penalty for failing to comply with a collection of information if it does not display a currently valid OMB control number. PLEASE DO NOT RETURN YOUR FORM TO THE ABOVE ADDRESS.

1. REPORT DATE (DD-MM-YYYY) 07-04-2003	2. REPORT TYPE EXECUTIVE ORDER	3. DATES COVERED (FROM - TO) xx-xx-2003 to xx-xx-2003	
4. TITLE AND SUBTITLE SURVIVABILITY MODELING AND VALIDATION IN COMPLEX RIB-SKIN STRUCTURES Unclassified		5a. CONTRACT NUMBER	
		5b. GRANT NUMBER	
		5c. PROGRAM ELEMENT NUMBER	
		5d. PROJECT NUMBER	
		5e. TASK NUMBER	
		5f. WORK UNIT NUMBER	
6. AUTHOR(S) BURKHARDT, JOHN ; JOYCE, PETER J ;			
7. PERFORMING ORGANIZATION NAME AND ADDRESS UNITED STATES NAVAL ACADEMY 590 HOLLOWAY RD. ANNAPOLIS, MD21402		8. PERFORMING ORGANIZATION REPORT NUMBER	
9. SPONSORING/MONITORING AGENCY NAME AND ADDRESS 		10. SPONSOR/MONITOR'S ACRONYM(S) AIAA	
		11. SPONSOR/MONITOR'S REPORT NUMBER(S) AIAA-2003-1470	
12. DISTRIBUTION/AVAILABILITY STATEMENT APUBLIC RELEASE			
13. SUPPLEMENTARY NOTES 44TH AIAA/ASME/ASCE/AHS STRUCTURES, STRUCTURAL DYNAMICS, AND MATERIALS CONFERENCE 7-10 APRIL 2003			
14. ABSTRACT THIS PAPER PRESENTS A COORDINATED EFFORT TO MODEL, TEST AND VALIDATE THE STRUCTURAL RESPONSE OF COMPLEX AEROSPACE RIB-SKIN STRUCTURES IN BOTH UNDAMAGED AND DAMAGED CONFIGURATIONS. COORDINATED EXPERIMENTAL AND FINITE ELEMENT MODEL RESULTS ARE PRESENTED FOR CYLINDRICAL RIB-SKIN STRUCTURES EACH APPROXIMATELY NINE FOOT LONG, AND THIRTY INCHES IN DIAMETER. THE TEST ARTICLES CONSIDERED ARE OF RIVETED ALUMINUM CONSTRUCTION AND INCLUDE INTERNAL STRUCTURAL STIFFENERS.			
15. SUBJECT TERMS MODELING;STRUCTURE;RIB;SKIN;COMPUTER SIMULATION;TESTING;STRAIN VERSUS LOAD;HYSTERESIS PLOT;DISPLACEMENT VERSUS LOAD;FEA;FINITE ELEMENT ANALYSIS;FINITE ELEMENT METHOD			
16. SECURITY CLASSIFICATION OF:		17. LIMITATION OF ABSTRACT Same as Report (SAR)	18. NUMBER OF PAGES 8
a. REPORT Unclassified	b. ABSTRACT Unclassified	c. THIS PAGE Unclassified	19. NAME OF RESPONSIBLE PERSON EGNER, DONNA DEGNER@BAH.COM
			19b. TELEPHONE NUMBER International Area Code Area Code Telephone Number 937255-3828 DSN 785-3828

traditional bending rig would produce a load state including spurious axial, bending or torsional loads inconsistent with pure cantilever bending. Such a test would be inconsistent with the load state assumed in the computer simulation and, therefore, would be a poor candidate for validation. In order to produce cantilever bending in asymmetric specimens, and therefore results suitable for validation of the computer models, a new bending rig was designed and constructed capable of compensating for lateral deflections.

Bending Rig and Test Fixture

A variety of bending rig designs were considered. The most obvious solution was to rigidly fasten the fixed end of the structures to a stiffened test frame and then load the free-end with dead weights. This would allow the free-end of the structure to deflect unconstrained, producing pure cantilever bending. Load controlled testing was rejected, however, as it would result in unstable, potentially catastrophic and dangerous failures. Considering that failure load estimates from the finite element analyses ranged from three thousand to ten thousand pounds the uncontrolled failure of a structure was deemed unacceptable. Consequently, a more controllable, displacement-controlled test rig design was sought.

Instead a displacement controlled test rig was designed. In this scheme a fixed displacement is applied to the structure, controlled by the operator, often per unit time, which, in turn, generates a force in the structure. In this displacement control there is little danger of losing control of the test article, if the



Figure 1. Runway beams, bridge beam and left and right end trucks.

specimen suddenly fails, the load is relieved but the displacement remains a constant until the operator makes a change. The complication, however, is to create a displacement controlled bending rig which also allows for tip deflections both lateral and longitudinal. The solution used in this study was to invert a bridge crane, which is normally mounted to the ceiling, and mount it to the floor. A typical bridge crane, Figure 1, is composed of two runway beams, two end trucks, a bridge beam and a trolley, Figure 2, which traverses the bridge beam.

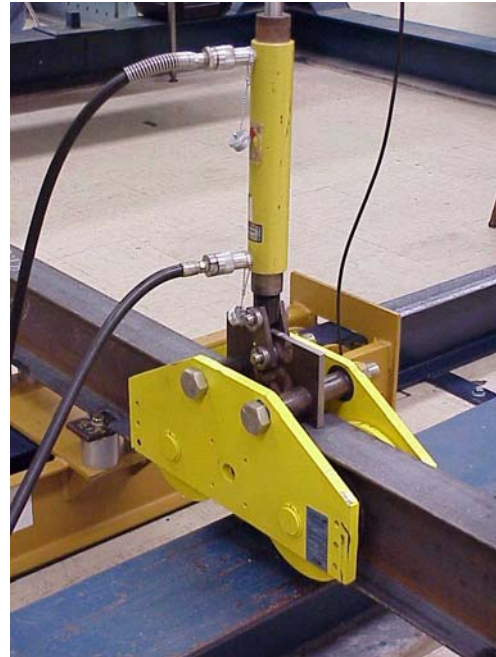


Figure 2. Bridge beam and trolley.

The structure being tested is positioned equidistant between the end trucks and fixed rigidly at one end. The end trucks can then be positioned along the runway beams so that the bridge beam lies directly below the load point on the structure. Consequently, the bend rig is capable of accommodating a wide range of structures. Most importantly, however, during loading if the load point on the structure moves perpendicular to the line of action of the applied load the hydraulic cylinder is capable of tracking the motion by the traversing along the bridge beam on the trolley with little resistive force.

Loads were applied to the structures using a sheet metal harness fixed to the free end of the test article with clevises on either side. The harness was attached to a link plate using a length of chain. A 20 kip load cell was pin connected to the link plate and then fixed to the hydraulic actuator as shown in Figure 3.

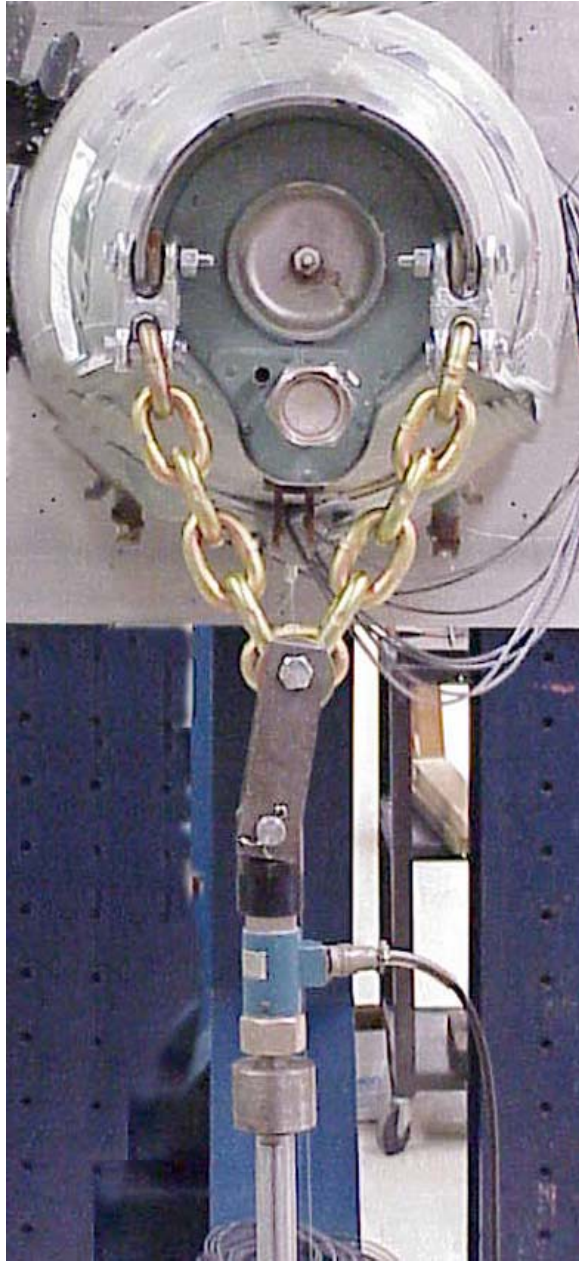


Figure 3. Loading harness and load cell.

Loads were applied to the structure using a 10-ton, long stroke, double-acting Enerpac hydraulic cylinder driven by a hand actuated hydraulic pump.

The test articles were mounted to the load frame, Figure 4, by a custom built test fixture. As designed the test fixture provides complete support for the fixed end of the test articles all the way around the circumference. To accomplish this an aluminum base plate was machined to attach to the load frame and then a ring of twenty four 3 in. x 3 in. x 6 in. long fixture blocks were attached to the base plate in an annular ring

using two 1/4-20 cap screws. Once attached the fixture blocks were machined into a circular pattern using a CNC mill to fit the test article, Figure 5. The machining pattern was based on measurements of the interior circumference of the test articles at the fore end and was rehearsed prior to cutting metal by machining a plywood plug. This manufacturing technique was chosen to reduce material waste and minimize machining time necessary to fabricate the loading ring. The loading ring was then fitted to the test article and bolted tight at each location using 1/4-20 cap screws bolted through a carefully fitted steel collar designed to distribute the load around the circumference of the test article.



Figure 4. Load frame before mounting test article.

Testing and Data Acquisition

In addition to the 20 kip load cell discussed above each structure was instrumented along the length for deflection and around the exterior for strain in the skin as shown below, Figure 6. Deflections were measured at locations along the length of the specimen (at the free end where the load was applied, at approximately $L/4$ and $L/2$) using Celesco Model PT101 string potentiometers with a 5 in. full range. Strain gages 1-7 to measure the flexural strains were installed along the ventral axis of the test article, evenly

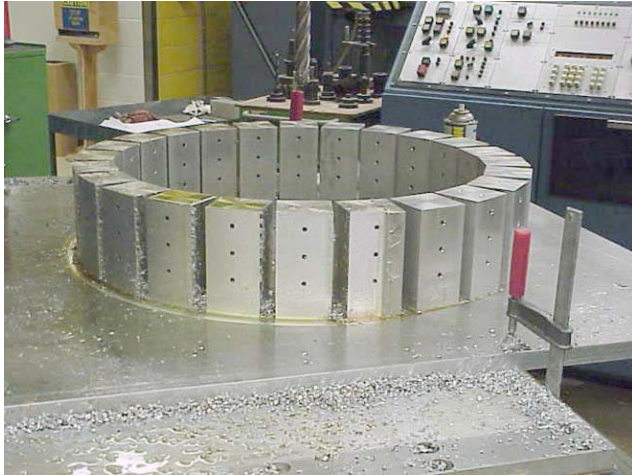


Figure 5. Fixture machining.

space from the free end to approximately $L/2$. Strain gages 8 and 9 were installed along the midline of the test article at approximately $L/2$, to measure the axial strain and the hoop strain at the midline. Strain gage 10 was installed on the dorsal axis approximately $L/5$ from the fixed end of the test article to measure the flexural strain. All of the strain gages were single pattern 120 Ω CEA-13-250UW-120 type gages from MicroMeasurements.

The specimens were loaded in 1000 lb increments and at each load step the load, displacement, and strain data was recorded using a Hewlett Packard 3852S Automatic Data Acquisition/Control System

together with a PC A/D card to generate a digital test log for each test. Tip deflections both lateral and longitudinal were measured by recording the movement of the trolley and the bridge beam using a tape measure at each load increment. Preliminary observations suggested negligible tip deflections in both the lateral and longitudinal directions.

Prior to each test the entire loading rig was raised off the floor using bottle jacks to support the weight of the load train, the trolley, and the bridge beam. After balancing the load cell, with the load train unloaded, the load train was engaged with the Enerpac hydraulic actuator fully extended so that the entire 10 inch stroke could be used for testing.

Initial tests of the loading rig showed little hysteresis in either the strain/load data or the displacement/load data (see Figure 7 and 8.) The data in Figure 7 and 8 was collected during loading and unloading of one of the test articles in the elastic range.

Typical displacement/load data and strain/load to failure are included in Figures 9 and 10. Figure 9 shows the expected pattern of increasing deflection with increased load becoming non-linear in this instance at or before 2500 lbs, which proved to be the onset of buckling in the skin. Also as expected we observed and decreased vertical deflection at $L/4$ and $L/2$, both points closer to the fixed end of the test article. Figure 10 exhibits a similar pattern of increasing flexural strain along the ventral axis of the

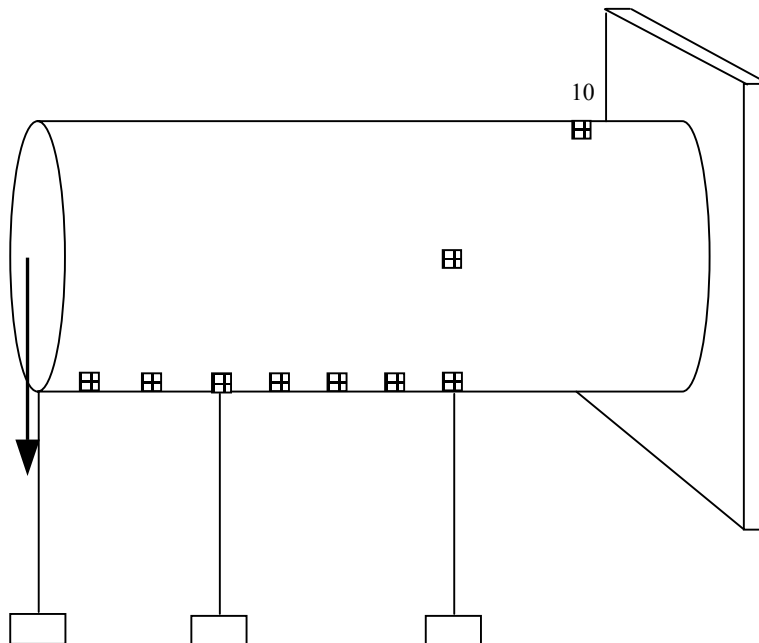


Figure 6. Strain gage and string potentiometer schematic.

test article with increasing load finally resulting in a dramatic divergence of the strains at strain gage location 4 at approximately 2500 lbs load. Post mortem inspection of the test article showed skin buckling in the vicinity of strain gage 4.

Analytical Model

Concurrent with the design and construction of the bending rig, a second research team constructed and analyzed finite element models to determine the mechanical response of both the damaged and undamaged structures in bending. The finite element

models were created based on detailed measurements of the actual structures. The structural geometry was created and meshed in ANSYS with ANSYS Shell 91 eight-noded elements, with six degrees of freedom at each node, to obtain a continuous, one-section structure. The finite element models developed included the aluminum metal sheet (outer skin) wrapped around aluminum z-angles (ribs) of the structure. The model does not account for its riveted construction or integral complexities.

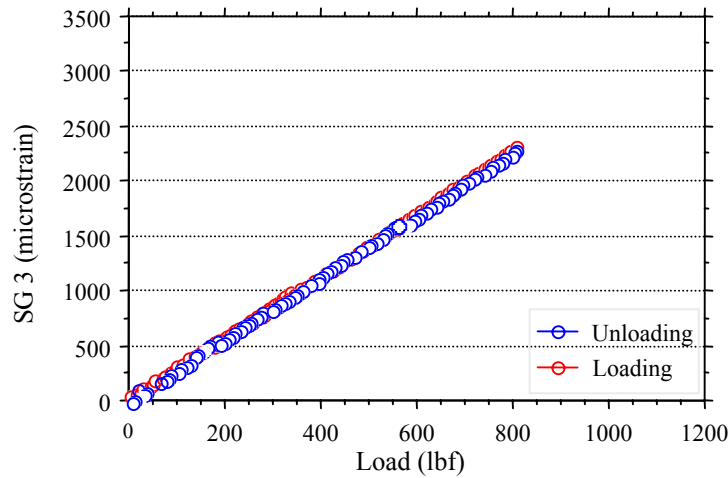


Figure 7. Strain versus load hysteresis plot.

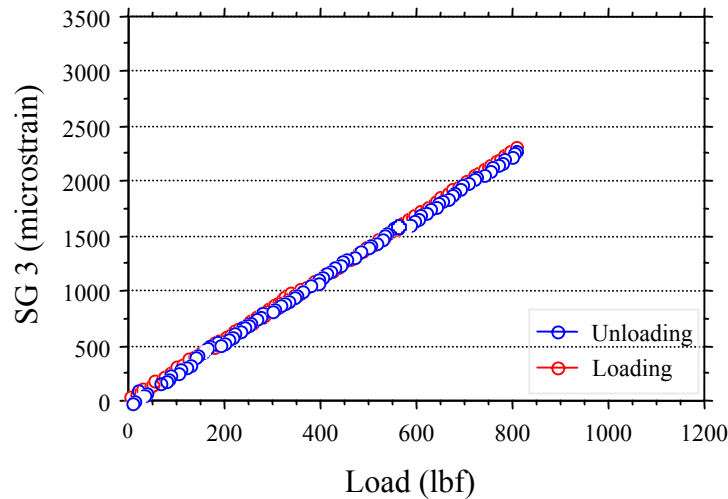


Figure 8. Displacement versus load hysteresis plot.

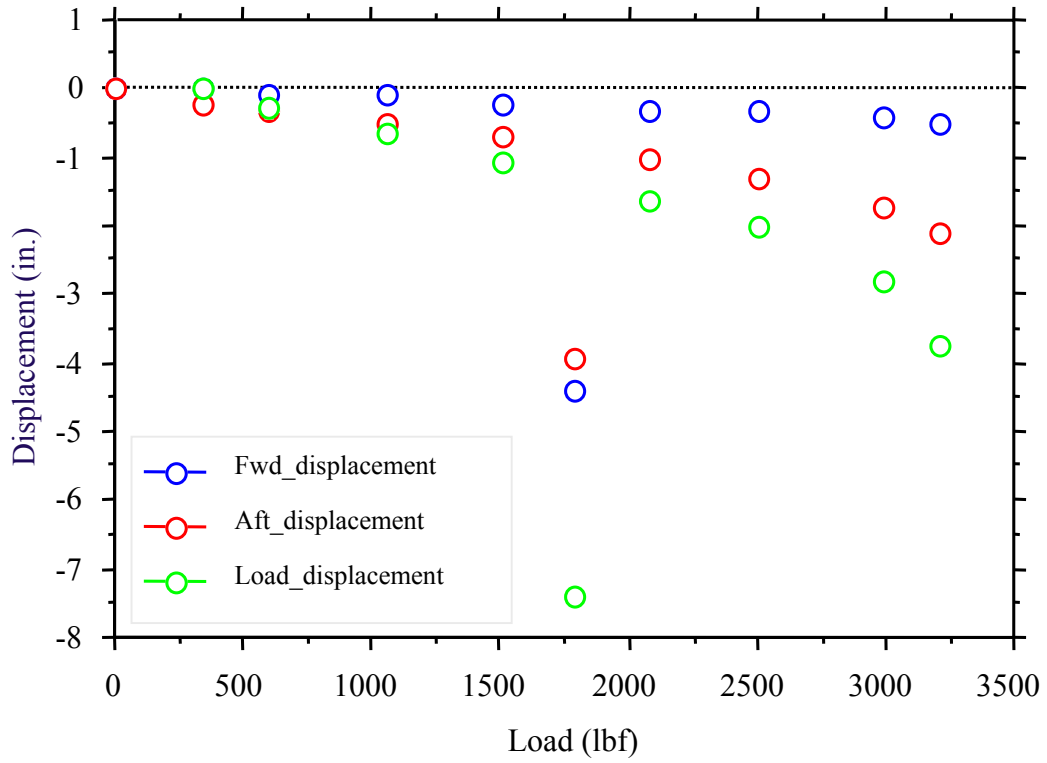


Figure 9. Displacement versus load.

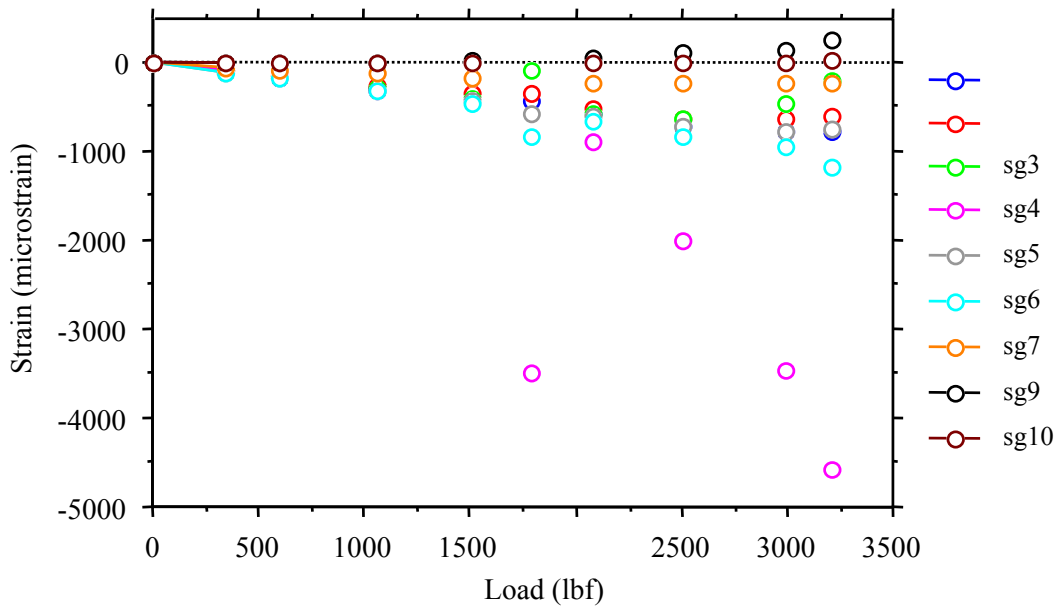


Figure 10. Strain versus load.

The models were solved quasi-statically in ANSYS using a linear material model and small deflection geometric constraints. Consequently, all finite element results are limited to small deflections and strains.

Summary and Comparison

Comparisons of test data with the finite element analysis results have shown very good agreement. As shown in Figure 11 the finite element analysis prediction for the undamaged target matches well with test data for a strain gage location close to the aft end (sg4) on the ventral surface. Additionally, the bending stiffness of the structure is well predicted by the finite element analysis whose prediction differs by only 1.02% from the experimentally determined value. The bending stiffness of the damaged structure was also accurately predicted by the finite element analysis up to the onset of buckling as shown in Figure 12. Moreover, in the damaged structure the bending stiffness has been reduced by 48% with respect to the undamaged

structure suggesting a resultant decrease in airworthiness and survivability.

The accuracy of the finite element analyses is, as expected, suspect at larger strains and deflections as indicated in the data for a damaged structure as in Figure 12. The restriction of the finite element model to small deflections and strains renders it incapable of predicting the complex behavior observed during the testing of the damaged structure. The finite element analysis shows good correlation with measured loads up to approximately 2,500 lbs. At larger loads, however, the structure began to fail due to buckling of the skin. Because of the buckling, the load paths through the structure are redistributed resulting in a discrepancy between measured and predicted strains. This is an area where the analysis falls short, since the limitations of the finite element model fidelity, such as missing interior components, prevented a prediction of where and at what load the structure would fail.

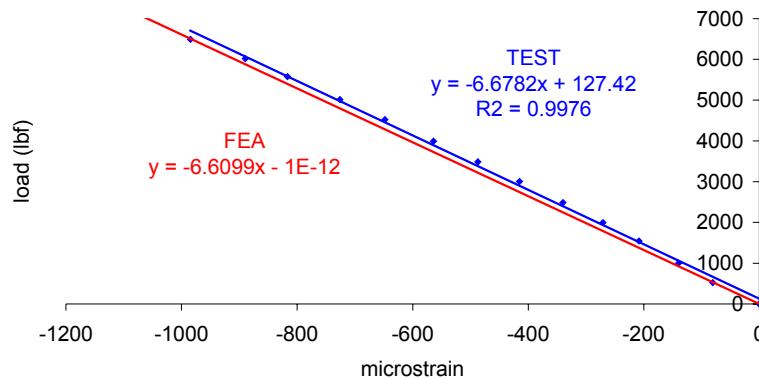


Figure 11. Experimental (—) vs. predicted FEA (—) response for undamaged structure.

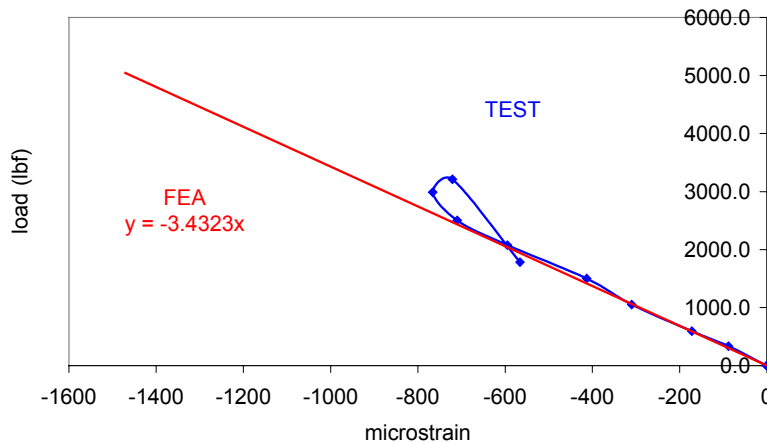


Figure 12. Experimental (—) vs. predicted FEA (—) response for damaged structure.

Conclusions

The results of this paper demonstrate the ability to model the behavior of complex rib-skin structures using the finite element method. Using a specially developed cantilever bending rig experimental results were obtained for complex asymmetric rib-skin structures typical of aerospace applications both undamaged and damaged that validated the small deflection, linear elastic finite element results. Because of the limitations of the finite element models used they were unable to accurately predict the failure modes in the damaged structure. The inability to predict failure is primarily due to the practical limitations on time and resources required to generate the fidelity necessary to accurately model the structure. Future efforts will concentrate on overcoming these limitations.